Deep Learning Enabled Slow Fluid Antenna Multiple Access

Noor Waqar, *Student Member, IEEE,* Kai-Kit Wong, *Fellow, IEEE,* Kin-Fai Tong, *Fellow, IEEE,* Adrian Sharples, and Yangyang Zhang

***Abstract*—The increasing interest of fluid antenna systems is reinforced by an unprecedented way of achieving multiple access, by exploiting moments of deep fades in space. This phenomenon, referred to as fluid antenna multiple access (FAMA), allows the fluid antenna at each user to be switched to a location in space (i.e., port) where the sum-interference power collectively suffers from a deep fade, resulting in a decent signal reception without the need of complex signal processing. Nevertheless, selecting the best port is an arduous task, which requires a large number of channel observations to obtain the high performance gain. This letter aims to devise a low-complexity port selection scheme for FAMA where each user has a small number of port observations only. We assume slow FAMA (s-FAMA) so that the selected port remains unchanged until the channel conditions change. A deep learning approach is proposed to infer the signal-to-interference plus noise ratios (SINR) at all the available ports given only a small number of observations. The simulation results exhibit that the proposed scheme is able to attain significant reductions in outage probability, and improvements in multiplexing gain, from a relatively small number of available port observations, showing great potential for future multiple access technologies.**

***Index Terms*—Deep learning, Fluid antenna, Multiple access, Multiuser communications, Slow FAMA.**

I. Introduction

THE explosive growth of smart devices and an increasing influx of new applications have sparked a paradigm shift in wireless communication networks. Such an upsurge is also coupled with the advances in mobile communication technology, from multiuser multiple-input multiple-output (MIMO) in fourth generation (4G) to massive MIMO in fifth generation (5G) networks [1]. The strength of MIMO originates from its unique ability to create artificial signal peaks as well as nulls by mixing multipath signals intelligently, essentially creating bandwidth out of space and enabling multiple access entirely in the spatial domain when multiple antennas are employed at the base station (BS) and/or user equipment (UE), resulting in extraordinary capacity and performance gains.

Even though MIMO has been standardized as a quintessential element of almost all future communication networks, it suffers from the drawback of sophisticated signal processing requirements in order to support more users. Though massive MIMO alleviates this issue to some extent by utilizing the law of large numbers and increasing the number of BS antennas to 64 in 5G, the number of BS antennas needs to be much greater than the number of UEs [2]. This motivates us to search for alternative methods to reap the benefits from spatial diversity in a much simpler way. One emerging technology attempting to achieve this goal is fluid antenna system [3], [4].

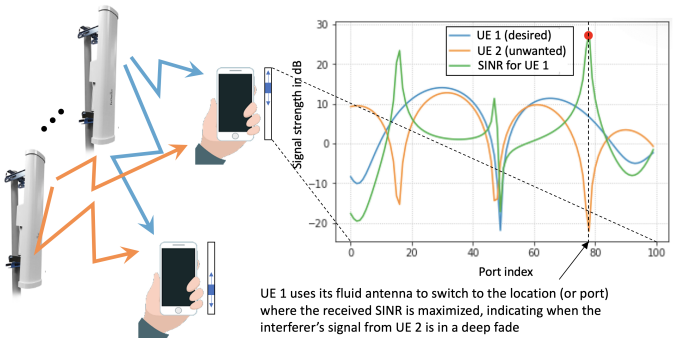

Fig. 1. An illustration for a two-user FAMA system in the downlink.

Fluid antenna system refers to a new type of antenna that is able to alter its shape and/or position dynamically to extract the best signal in space. This is made possible by the advent of liquid antennas [5] and reconfigurable pixel antennas [6], [7] in recent years. Early studies on considering such position-adaptable antenna for single-user channels were given in [8], [9], demonstrating great diversity and capacity benefits. Since then, researchers have stepped up in studying the performance of fluid antenna systems in more general fading channels [10]–[12] and designing new coded modulation schemes [13].

Remarkably, a rather surprising result is that multiple access becomes possible by accessing to the natural interference null in a small space through a position-adaptable fluid antenna at each user. This approach is referred to as *fluid antenna multiple access (FAMA)* [3] and was first presented in [14]. As shown in Fig. 1, two users can be served on the same channel in the downlink by having each BS antenna transmitting to one of the users and each user has a fluid antenna to scan the entire fading envelope in its space, and switch to the position (i.e., port) where the interference signal disappears naturally due to multipath fading. FAMA with more users is also possible.

Specifically, it can be a fast FAMA (f-FAMA) system which requires each fluid antenna to switch to the best port on a symbol-by-symbol basis to exploit the sum-interference *signal* null [14] whereas a more practical approach is the slow FAMA (s-FAMA) scheme that switches to the sum-interference plus

The work is supported in part by the Engineering and Physical Sciences Research Council (EPSRC) under Grant EP/W522077/1 for an Industrial CASE studentship with project number 2646370. For the purpose of open access, the authors have applied a Creative Commons Attribution (CC BY) licence to any Author Accepted Manuscript version arising.

N. Waqar, K. Wong and K. Tong are with the Department of Electronic and Electrical Engineering, University College London, Torrington Place, WC1E 7JE, United Kingdom. Corresponding author: kai-kit.wong@ucl.ac.uk.

A. Sharples is with British Telecommunications.

Y. Zhang is with Kuang-Chi Science Limited, Hong Kong SAR, China.

noise *power* null. The latter only needs to switch the port of fluid antenna when the channel changes [3]. FAMA reduces multiple access to a simple port searching task at the UE side without precoding and channel state information (CSI) at the BS. In this letter, our focus is on the s-FAMA system.

However, how to choose the best port is still a challenging problem. This is because s-FAMA generally requires a large number of switchable positions (or ports) to exploit the deep fades occurring in narrow regions but acquiring observations at all the ports is infeasible. Similar to [15], this letter leverages deep learning to infer the best port given only a few observations over the ports. Nonetheless, one fundamental difference is that [15] investigated a single-user system while this letter addresses the multiuser s-FAMA network. In particular, [15] attempts to estimate the UE's channel envelopes of all the ports whereas this work's objective is to estimate the average signal-to-interference plus noise ratios (SINRs) over the ports. Another major difference is that this letter uses a more accurate channel model to emulate the spatial correlation over the ports, showing more importance on the size than resolution of fluid antenna, contrary to the results in [15]. Our main contribution is a deep learning method that can infer the SINR at all the ports from a few observations for selecting the best port for s-FAMA. Simulation results will demonstrate that the proposed scheme is able to obtain near-optimal performance, with just $15-20\%$ of the ports observed. Remarkably, s-FAMA can serve 5 users, achieving a multiplexing gain of 4.

II. System Model

A. The s-FAMA Network

We consider a downlink system as shown in Fig. 1, where a multi-antenna BS is adopted to transmit messages to U user equipments (UEs) on the same time-frequency resource unit.[1] The BS employs fixed antennas, each of which is responsible for transmitting messages to one of the UEs while each UE is equipped with a fluid antenna occupying a linear space of $W\lambda$ in which λ is the wavelength. The fluid antenna has N ports,[2] the positions evenly distributed over the space, to which its radiating element can be switched instantly. Each port is assumed to behave like an ideal point antenna, meaning that each UE has the ability to effectively switch its antenna to one of the N positions to optimize its performance.

The received signal at the k-port of UE u is given by

$$y_k^{(u)} = g_k^{(u,u)} s_u + \sum_{\substack{\tilde{u}=1 \\ \tilde{u}\neq u}}^{U} g_k^{(\tilde{u},u)} s_{\tilde{u}} + \eta_k^{(u)}, \tag{1}$$

where $g_k^{(\tilde{u},u)}$ denotes the channel from the $\tilde{u}$-th BS antenna to the k-th port of UE u, s_u is the information symbol intended for UE u, with $\mathrm{E}[|s_u|^2] = \sigma_s^2$, and $\eta_k^{(u)}$ denotes the zero-mean complex Gaussian noise at the k-th port of UE u with variance of σ_η^2. Also, U denotes the number of UEs.

[1]The proposed s-FAMA approach in fact can be directly applied even if the UEs are served by different BSs because no preprocessing or precoding is required from the BS side and the UEs operate exactly in the same way.

[2]Mutual coupling does not exist among the ports in a liquid-based fluid antenna because there is always only one radiating element. Note also that fluid antenna does not suffer more non-ideal effects such as radiation pattern, cross-polarization interference and etc. than conventional fixed antennas.

B. Channel Model

All of the channels are assumed to be zero-mean complex Gaussian so that the amplitude, $|g_k^{(\tilde{u},u)}|$, follows a Rayleigh distribution, with probability density function (pdf)

$$p_{|g_k^{(\tilde{u},u)}|}(r) = \frac{2r}{\sigma^2} e^{-\frac{r^2}{\sigma^2}}, \text{for } r \geq 0, \text{with } \mathrm{E}[|g_k^{(\tilde{u},u)}|^2] = \sigma^2. \tag{2}$$

Since $\{g_k^{(\tilde{u},u)}\}_{\forall k}$ correspond to the channels at closely located ports, they can be very strongly correlated. In [15], [16] and all other related works, a so-called generalized channel model which was originated from [17], was employed to maintain mathematical tractability. Nonetheless, the model actually has a very limited degree of freedom (DoF) to control the spatial correlation between the channels. Different from the previous works, we propose to model $g_k^{(\tilde{u},u)}$ by

$$\begin{bmatrix} g_1 \\ g_2 \\ \vdots \\ g_N \end{bmatrix} = \begin{bmatrix} a_{11} & a_{12} & \cdots & a_{1N} \\ a_{21} & a_{22} & \cdots & a_{2N} \\ \vdots & & \ddots & \vdots \\ a_{N1} & \cdots & & a_{NN} \end{bmatrix} \begin{bmatrix} x_1 \\ x_2 \\ \vdots \\ x_N \end{bmatrix} \tag{3}$$

$$\Longleftrightarrow \boldsymbol{g} = \mathbf{A}\boldsymbol{x}, \tag{4}$$

in which the superscript $(\tilde{u},u)$ has been omitted for conciseness, $\{x_k\}_{k=1}^N$ are independent, identically distributed (i.i.d.) standard complex Gaussian random variables, and $\mathbf{A}$ plays the role of ensuring that the channels, $\boldsymbol{g}$, have the necessary cross-correlation structures. For a line-shaped fluid antenna of length $W\lambda$ in a rich, 2D isotropic scattering environment, the cross-correlation of the channels between any two ports is known to follow the Jake's model [18] and given by

$$\mathrm{E}[g_k g_\ell^*] = \phi_{k,\ell} = \sigma^2 J_0\left(\frac{2\pi(k-\ell)W}{N-1}\right). \tag{5}$$

Defining $\mathbf{\Phi} \triangleq [\phi_{k,\ell}]$ and with (5), we require

$$\mathbf{\Phi} = \mathrm{E}[\boldsymbol{g}\boldsymbol{g}^\dagger] = \mathbf{A}\mathbf{A}^\dagger, \tag{6}$$

where $\boldsymbol{g} \triangleq [g_1 \cdots g_N]^T$. Using eigenvalue decomposition, we write $\mathbf{\Phi} = \mathbf{V}\mathbf{D}\mathbf{V}^\dagger$ where $\mathbf{D}$ is a diagonal matrix containing the eigenvalues and $\mathbf{V}$ is a unitary matrix of eigenvectors. As a result, $\mathbf{A}$ can be chosen as $\mathbf{A} = \mathbf{V}\mathbf{D}^{\frac{1}{2}}$ to meet (5).

C. Port Selection Maximizing SINR

At each UE, say u, the SINR at the k-th port is given by

$$\gamma_k^{(u)} = \frac{\sigma_s^2 |g_k^{(u,u)}|^2}{\sigma_s^2 \sum_{\substack{\tilde{u}=1 \\ \tilde{u}\neq u}}^{U} |g_k^{(\tilde{u},u)}|^2 + \sigma_\eta^2}. \tag{7}$$

To achieve s-FAMA, UE u finds and switches to the port, k^*, that maximizes the SINR, i.e.,

$$k^* = \arg\max_k \gamma_k^{(u)}. \tag{8}$$

Given a target SINR, γ_{th}, the reception performance can be characterized by the outage probability

$$p_{\mathrm{out}} = \mathrm{Prob}\left(\gamma_{k^*}^{(u)} = \max_k \gamma_k^{(u)} < \gamma_{\mathrm{th}}\right). \tag{9}$$

With i.i.d. UEs,[3] the capacity scaling can be measured through the multiplexing gain which is found as

$$m = U(1 - p_{\text{out}}). \tag{10}$$

III. Low-complexity Deep Learning-based Port Selection

A. SINR-based Utility Inference

If $\{\gamma_k^{(u)}\}_{k=1}^N$ are all known, then the maximization of SINR is straightforward. In s-FAMA, however, N is supposed to be large, e.g., $N = 100$, in order to have sufficient resolution to resolve the interference. This means that obtaining the SINR at all N ports is unviable, and in practice, the SINR of only a small subset of the ports will be available. The UE will need to estimate the SINR of the unobserved ports in order to find the best port for maximizing the overall SINR. Denoting $\mathcal{P}$ as the set containing the indices of the observed ports and $\mathcal{Q}$ as that of the unobserved ports, UE u aims to find

$$\tilde{k}^* = \arg_k \max \left\{ \{\gamma_k^{(u)}\}_{k\in\mathcal{P}}, \{\tilde{\gamma}_k^{(u)}\}_{k\in\mathcal{Q}} \right\}, \tag{11}$$

where $\tilde{\gamma}_k^{(u)}$ is the estimate of the SINR at the k-th port.

To achieve (11), our objective is to develop an approach to infer the SINR of the *unobserved* ports based on the SINR of the observed ports by utilizing the spatial correlation over the ports, which we will address in the next subsection.

B. Long Short Term Memory (LSTM) for SINR Estimation

Deep learning techniques have recently received considerable interest and are being widely utilized in applications, such as channel estimation [19] and tracking [20]. The strength of deep learning lies in its ability to extract useful patterns and information from data without any prior knowledge about the characteristics of the data and environment. To track the space-varying characteristics, as in our case, it is important to give the neural networks an ability to learn the correlation across the spatial domain. Recurrent neural networks and LSTM are two widely considered methods for solving these tasks.

As an enhancement of recurrent neural networks, LSTM is a gradient-based learning method which is able to connect previous information to current task [21]. LSTM can deal with long-term dependencies, which improves the capacity of the network to process data. We exploit this property of LSTM to consider the SINR information over the ports as a time (space) series, to estimate the received SINR at the unobserved ports. The LSTM model is stacked with supervised learning to train using mean-squared error (MSE) as the loss function

$$\mathcal{L}_{\text{MSE}} = \mathbb{E}\left[\frac{1}{|\mathcal{Q}|} \sum_{k\in\mathcal{Q}} (\gamma_k^{(u)} - \tilde{\gamma}_k^{(u)})^2 \right], \tag{12}$$

where the expectation is taken over all the examples in the dataset. Moreover, we employ a bidirectional LSTM structure to combine both forward and backward directions to utilize both prior and future information. TABLE I summarizes the key parameters of the LSTM network we use.

[3]The proposed approach works in the same way even if the assumption does not hold. This assumption is adopted to simplify discusion.

TABLE I
LSTM Network Settings

Parameter	Value
Layer 1	50 LSTM cells (Bidirectional); Rectified Linear Unit (ReLU); shape = $(\lvert\mathcal{P}\rvert, 1)$
Layer 2	50 LSTM cells (Bidirectional); Rectified Linear Unit (ReLU)
Layer 3	Dense (Time distributed); $\lvert\mathcal{Q}\rvert$ neurons
Batch size	128
Epochs	50
Optimizer	ADAM with MSE as loss function
Learning rate	0.001

At each UE, the channel samples for the N-port fluid antenna were generated according to the statistical distributions in Section II-B. The samples were divided into 'observed' and 'estimated' channels using the scheme in [15]. The observed channels are inputs to the LSTM network, while the estimated channels represent the outputs of the LSTM network. As the channel data were all simulated, the exact channels (i.e., the labelled data) of the to-be-estimated channel ports were known and used to train the LSTM network using supervised learning.

LSTM, by default, takes a three-dimensional array as input, which is composed of the batch-size (training examples), the number of time/space-steps (the number of observed ports), and the number of features (one in this case as only channel gains for one instance). In the same way, the LSTM network gives a two-dimensional output composed of the batch-size and the predicted time/space steps (estimated channel gains). Additionally, the methodology for dividing the data into training and validation sets, was the standard 70-to-30 ratio, with 70% of the generated data used for training, and 30% data for validation of the training process.

IV. Simulation Results

In this section, we present the simulation results to evaluate the performance of the proposed deep learning based s-FAMA system with U users, each of which employs an N-port fluid antenna of length $W\lambda$. All of the UEs have the same SINR threshold, γ_{th}. In the simulations, the average received signal-to-noise ratio (SNR) at each UE is set to 10dB. Besides the proposed technique labelled as 'Proposed' in the figures, two benchmarks are considered. The first is 'Ideal' which assumes availability of the SINR at all the ports for port selection while 'Reference' selects the best port only among those observed ports. In other words, 'Ideal' is the performance upper bound while 'Reference' is the performance lower bound.

Fig. 2 demonstrates an example indicating how the SINR estimation of the proposed method improves as the number of observed ports increases, for a 2-user s-FAMA system when $W = 2$ and $N = 100$ for the fluid antennas. As expected, the prediction performance improves if more ports are observed and interestingly, the results show that with only 25% of the ports observed, the proposed method can produce the SINR estimates almost perfectly, enough to be used for port selection for maximizing the SINR. For this reason, in the following, 'Proposed' refers to the proposed LSTM method for estimating SINR when only 20% of the ports are observed.

The results in Fig. 3 are provided for the outage probability of the fluid antenna systems with $N = 100$. First, we observe

This article has been accepted for publication in IEEE Communications Letters. This is the author's version which has not been fully edited and content may change prior to final publication. Citation information: DOI 10.1109/LCOMM.2023.3237595

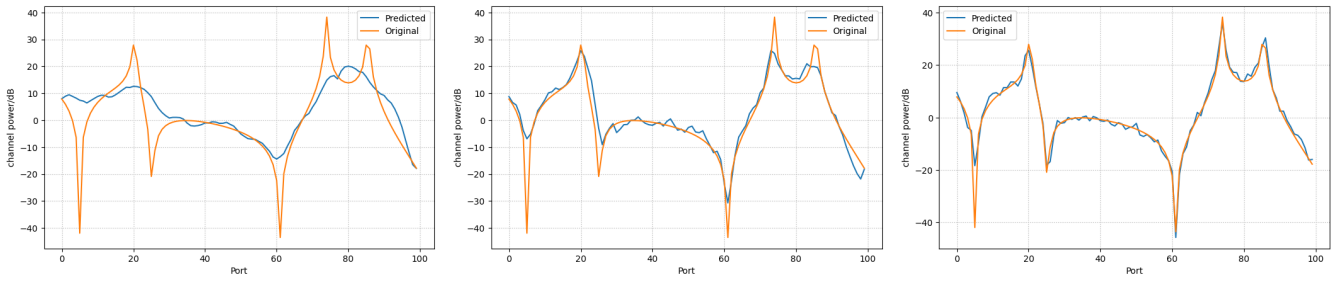

(a) 10 observed ports (b) 15 observed ports (c) 25 observed ports

Fig. 2. The SINR prediction performance of the proposed LSTM network when $W = 2$, $U = 2$ and $N = 100$.

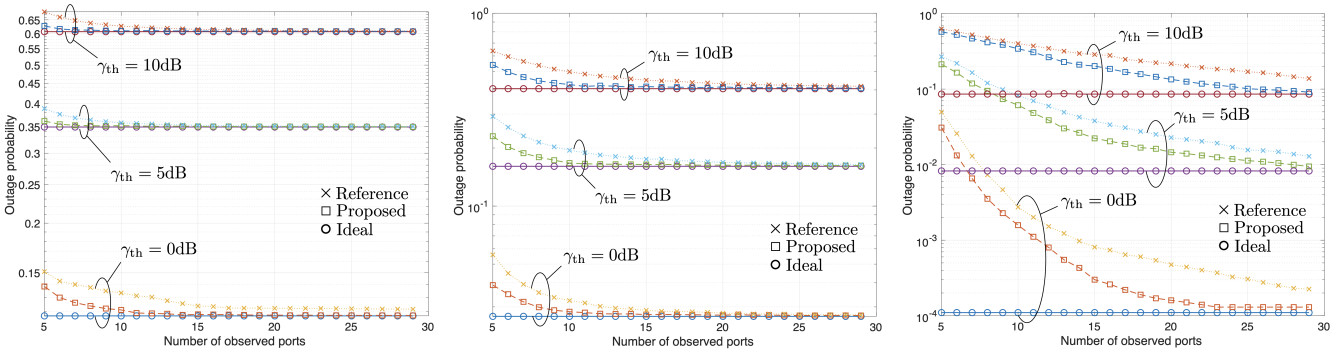

(a) $W = 0.5$ (b) $W = 1$ (c) $W = 3$

Fig. 3. Outage probability for 2-user s-FAMA systems against the number of observed ports for different $\gamma_{\rm th}$ when $N = 100$.

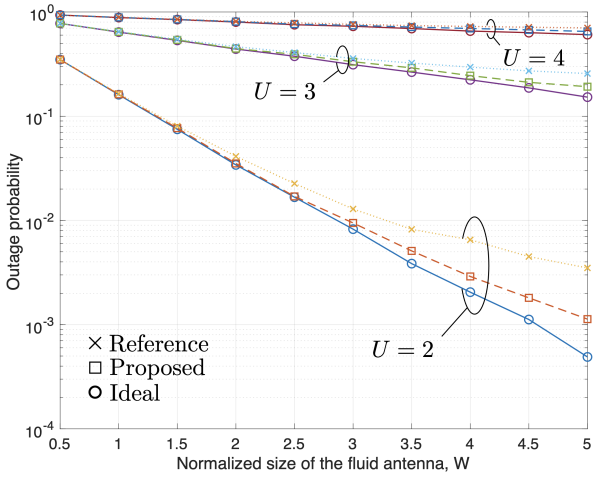

Fig. 4. Outage probability for the s-FAMA systems against the size of fluid antenna at each user, W, for different U with $N = 100$ and $\gamma_{\rm th} = 5$dB.

that when the number of observed ports increases, the outage probability decreases. Also, as expected, if the SINR threshold, $\gamma_{\rm th}$, increases, the outage probability will increase. The size, W, of each fluid antenna is another major factor that affects the outage probability. In particular, a larger W will considerably bring down the outage probability. Moreover, the performance difference between 'Proposed' and 'Reference' indicates the remarkable gains from utilizing the proposed LSTM approach. The results illustrate that with $25 - 30\%$ ports observed, our proposed method achieves performance very close to 'Ideal'.

Fig. 4 investigates the outage probability performance of the fluid antenna systems against the normalized size of each fluid antenna, W, when $N = 100$ and $\gamma_{\rm th} = 5$dB. As expected, increasing W lowers the outage probability and increasing the number of users, U, raises the outage probability.

While outage probability indicates the interference immunity of each user, the multiplexing gain of the network serves to quantify the capacity advantage over a single-user system occupying the same amount of bandwidth. In Fig. 5, the results are provided for the multiplexing gain of the fluid antenna systems when $W = 2$ and $\gamma_{\rm th} = 0$dB. As can be observed, the multiplexing gain grows with the number of ports and the proposed method converges to 'Ideal' very quickly although a system with more users will need a larger N to reach the capacity scaling of the 'Ideal' method. Additionally, the results show that s-FAMA does not need a large number of ports to support several users. In particular, we only need $N = 50$ ports to support $U = 4$ users achieving a multiplexing gain of close to 3.4 while a $U = 3$ user system needs only $N = 40$ ports at the fluid antenna to obtain a multiplexing gain of 2.85, close to the maximum capacity scaling for a 3-user system.

We conclude this section by considering the results in Fig. 6 where the multiplexing gain for the s-FAMA systems is plotted against the number of users for different W. In the figure, we have assumed that $N = 100$ and $\gamma_{\rm th} = 0$dB. First of all, we observe that the proposed method achieves nearly the same

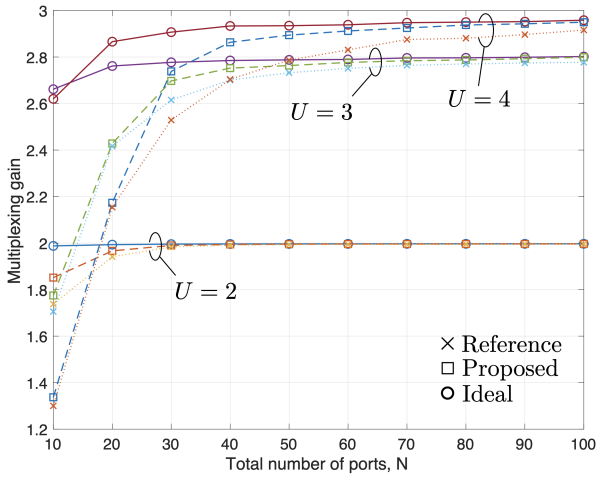

Fig. 5. Multiplexing gain for the s-FAMA systems against the number of ports at each fluid antenna, W, for different U, with $W = 2$ and $\gamma_{\rm th} = 0$dB.

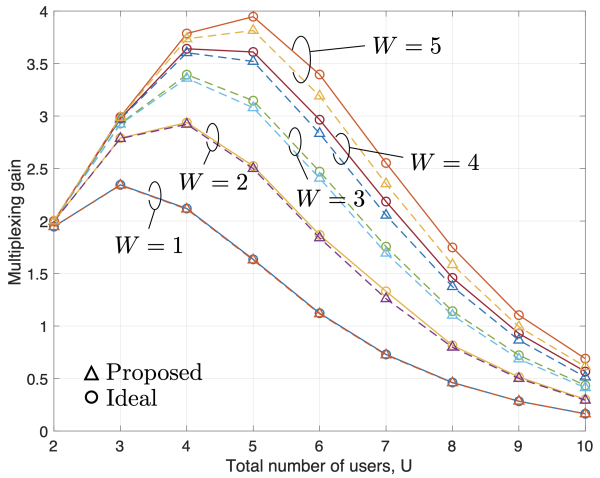

Fig. 6. Multiplexing gain for the s-FAMA systems against the number of users, U, for different W when $N = 100$ and $\gamma_{\rm th} = 0$dB.

performance as 'Ideal' although the difference gets slightly bigger when W is larger. In addition, the results demonstrate that the multiplexing gain of the s-FAMA systems begins to increase as the number of users increases but then reaches the maximum and starts to drop if the number of users continue to increase. The reason is that the multiplexing gain should rise with the number of users if the fluid antenna at each user is able to resolve the interference. However, when the number of users is too large, the outage probability at each user becomes very large and the network capacity begins to suffer. Despite this, the results indicate that s-FAMA can support 5 users on the same time-frequency resource and achieve more than 4 multiplexing gain (i.e., 4 times the capacity).

V. Conclusion

This letter proposed an LSTM-based port selection scheme for s-FAMA systems which exploited moments of deep fade of the interference to extract the best received signal. The proposed approach needed only a small number of correlated SINR observations, and yet could deliver near-maximal multiplexing gain performance. Our simulation results exhibited the effectiveness of the proposed scheme in reducing the outage probability and enhancing the multiplexing gain. The results further revealed that s-FAMA could support a large number of users for high multiplexing gain, without the need of precoding at the BS nor multiuser detection at each mobile user.

References

[1] E. G. Larsson, O. Edfors, F. Tufvesson and T. L. Marzetta, "Massive MIMO for next generation wireless systems," *IEEE Commun. Mag.*, vol. 52, no. 2, pp. 186–195, Feb. 2014.

[2] H. Q. Ngo, E. G. Larsson and T. L. Marzetta, "Energy and spectral efficiency of very large multiuser MIMO systems," *IEEE Trans. Commun.*, vol. 61, no. 4, pp. 1436–1449, Apr. 2013.

[3] K. K. Wong, K. F. Tong, Y. Shen, Y. Chen, and Y. Zhang, "Bruce Lee-inspired fluid antenna system: Six research topics and the potentials for 6G," *Frontiers in Commun. and Netw., section Wireless Commun.*, 3:853416, Mar. 2022.

[4] A. Shojaeifard *et al.*, "MIMO evolution beyond 5G through reconfigurable intelligent surfaces and fluid antenna systems," *Proc. IEEE*, 2022.

[5] Y. Huang, L. Xing, C. Song, S. Wang and F. Elhouni, "Liquid antennas: Past, present and future," *IEEE Open J. Antennas and Propag.*, vol. 2, pp. 473–487, 2021.

[6] D. Rodrigo, B. A. Cetiner and L. Jofre, "Frequency, radiation pattern and polarization reconfigurable antenna using a parasitic pixel layer," *IEEE Trans. Antennas and Propag.*, vol. 62, no. 6, pp. 3422–3427, Jun. 2014.

[7] S. Song and R. D. Murch, "An efficient approach for optimizing frequency reconfigurable pixel antennas using genetic algorithms," *IEEE Trans. Antennas and Propag.*, vol. 62, no. 2, pp. 609–620, Feb. 2014.

[8] K. K. Wong, A. Shojaeifard, K.-F. Tong and Y. Zhang, "Fluid antenna systems," *IEEE Trans. Wireless Commun.*, vol. 20, no. 3, pp. 1950–1962, Mar. 2021.

[9] K. K. Wong, A. Shojaeifard, K.-F. Tong and Y. Zhang, "Performance limits of fluid antenna systems," *IEEE Commun. Lett.*, vol. 24, no. 11, pp. 2469–2472, Nov. 2020.

[10] L. Tlebaldiyeva, G. Nauryzbayev, S. Arzykulov, A. Eltawil and T. Tsiftsis, "Enhancing QoS through fluid antenna systems over correlated Nakagami-m fading channels," in *Proc. IEEE Wireless Commun. Netw. Conf. (WCNC)*, pp. 78–83, 10-13 Apr. 2022, Austin, TX, USA.

[11] M. Khammassi, A. Kammoun, and M.-S. Alouini, "A new analytical approximation of the fluid antenna system channel," [Online] arXiv preprint arXiv:2203.09318, 2022.

[12] P. Mukherjee, C. Psomas, and I. Krikidis, "On the level crossing rate of fluid antenna systems," [Online] arXiv preprint arXiv:2205.01711, 2022.

[13] C. Psomas, G. M. Kraidy, K. K. Wong, and I. Krikidis, "On the diversity and coded modulation design of fluid antenna systems," [Online] arXiv preprint arXiv:2205.01962, 2022.

[14] K. K. Wong, and K. F. Tong, "Fluid antenna multiple access," *IEEE Trans. Wireless Commun.*, vol. 21, no. 7, pp. 4801–4815, Jul. 2022.

[15] Z. Chai, K. K. Wong, K. F. Tong, Y. Chen and Y. Zhang, "Port selection for fluid antenna systems," *IEEE Commun. Letters*, vol. 26, no. 5, pp. 1180–1184, May 2022.

[16] K. K. Wong, K. F., Tong, Y. Chen, and Y. Zhang, "Closed-form expressions for spatial correlation parameters for performance analysis of fluid antenna systems," *Elect. Lett.*, vol. 58, no. 11, pp. 454–457, 2022.

[17] N. C. Beaulieu and K. T. Hemachandra, "Novel simple representations for Gaussian class multivariate distributions with generalized correlation," *IEEE Trans. Inform. Theory*, vol. 57, no. 12, pp. 8072–8083, Dec. 2011.

[18] G. L. Stüber, *Principles of Mobile Communication*, Second Edition, Kluwer Academic Publishers, 2002.

[19] Y. Yang, F. Gao, X. Ma and S. Zhang, "Deep learning-based channel estimation for doubly selective fading channels," *IEEE Access*, vol. 7, pp. 36579–36589, 2019.

[20] J. Yu, X. Liu, Y. Gao, C. Zhang and W. Zhang, "Deep learning for channel tracking in IRS-assisted UAV communication systems," *IEEE Trans. Wireless Commun.*, vol. 21, no. 9, pp. 7711–7722, Sept. 2022.

[21] K. Greff, R. K. Srivastava, J. Koutnk, B. R. Steunebrink and J. Schmidhuber, "LSTM: A search space odyssey," *IEEE Trans. Neural Netw. Learning Syst.*, vol. 28, no. 10, pp. 2222–2232, Oct. 2017.